Baltic Astronomy, vol. 20, 453–458, 2011

A COMPLEX STELLAR LINE-OF-SIGHT VELOCITY DISTRIBUTION IN THE LENTICULAR GALAXY NGC 524

I. Katkov[1], I. Chilingarian[2,1], O. Sil'chenko[1], A. Zasov[1] and V. Afanasiev[3]

[1] *Sternberg Astronomical Institute, Moscow State University, Universitetskii pr. 13, Moscow, 119992, Russia;*

[2] *CDS – Observatoire de Strasbourg, CNRS UMR 7550, Université de Strasbourg, 11 Rue de l'Université, 67000 Strasbourg, France*

[3] *Special Astrophysical Observatory, Russian Academy of Sciences, Nizhnii Arkhyz, Karachaevo-Cherkesskaya Republic, 369167 Russia*

Received: 2011 August 8; accepted: 2011 August 15

Abstract. We present a detailed study of the stellar and gaseous kinematics in the luminous early-type galaxy NGC 524, derived from the long-slit spectroscopic observations obtained with the Russian 6 m telescope and the IFU data from the SAURON survey. The stellar line-of-sight velocity distribution (LOSVD) of NGC 524 exhibits strong asymmetry. We performed a comprehensive analysis of the LOSVD using two complementary approaches by the NBURSTS full spectral fitting technique: (a) a non-parametric LOSVD recovery and (b) a parametric recovery of two Gaussian kinematical components having different stellar populations. We discuss the origin of the complex stellar LOSVD of NGC 524.

Key words: galaxies: kinematics and dynamics: individual (NGC 524)

1. INTRODUCTION

NGC 524 is a luminous ($M_B = -21.7$ mag) lenticular galaxy settled in the center of a rich group (Garcia 1993) containing a X-ray hot gas component with a slightly lopsided distribution with respect to NGC 524 (Mulchaey et al. 2003). The galaxy demonstrates nearly circular isophotes, $\epsilon < 0.05$ (e.g., Magrelli et al. 1992), so from the photometric point of view it looks face-on. However, kinematic measurements revealed quite fast rotation of the galaxy (Sil'chenko 2000; Simien & Prugniel 2000; Emsellem et al. 2004) that is inconsistent with the photometric inclination of $< 18°$. Moreover, NGC 524 possesses a roundish disk of ionized gas extending up to 4 kpc (25 arcsec) from the center (Macchetto et al. 1996) rotating even faster than the stars. By comparing the rotation of the ionized gas and the stars in the center of NGC 524, Sil'chenko (2000) suggested that its gaseous disk is inclined with respect to the stellar one. The recent structural analysis of NGC 524 (Sil'chenko 2009) reveals that the bulge of this giant lenticular galaxy is rather modest and is seen only inside $R \approx 10''$, while the general structure is dominated by two exponential stellar disks with the scale-lengths of 0.9 and 3 kpc, respectively.

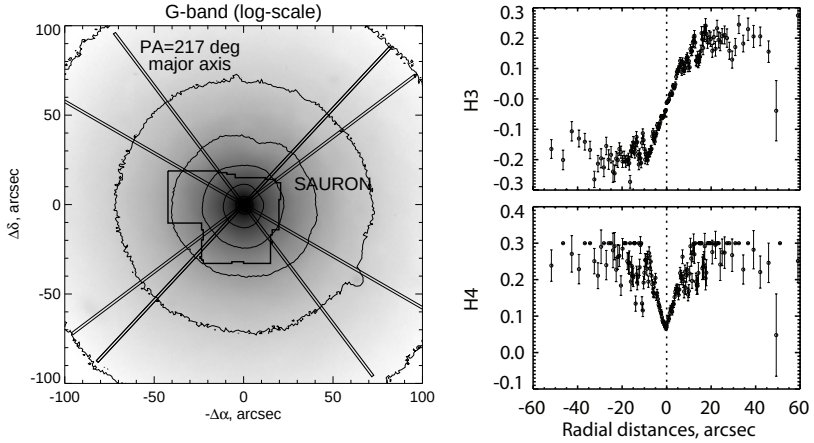

Fig. 1. Left panel. The positions of the SCORPIO slits and the SAURON mosaic field of view are overlapped onto the g-band image of NGC 524 obtained with CFHT. Right panel. The Gauss-Hermite coefficients characterizing the asymmetry of the stellar LOSVD.

2. OBSERVATIONS AND DATA REDUCTION

We used two datasets derived from long-slit and integral-field spectroscopy. The long-slit spectroscopic observations were obtained with the SCORPIO universal spectrograph (Afanasiev & Moiseev 2005) at the prime focus of the Russian 6 m BTA telescope of the Special Astrophysical Observatory. We observed NGC 524 in six slit positions (P.A. = 137, 217, 240, 295, 307, 317 deg, see Figure 1 (left panel) going through the galaxy center. Here we present only a long-slit spectrum obtained along the kinematical major axis (P.A. = 217°). We used the "green" (480–550 nm) and "red" (610–710 nm) spectral setups covering strong stellar absorption features as well as the emission lines of the ionized gas, $H\beta$, [O III] ($\lambda =$ 4959 and 5007 Å), $H\alpha$, [N II] ($\lambda = 6548$ and 6583 Å), [S II] ($\lambda = 6716$ and 6731 Å) providing the spectral resolution of 0.22 nm and 0.31 nm, respectively.

Data reduction for the long-slit spectral data of NGC 524 was identical to that of the lenticular galaxy NGC 7743 presented in Katkov et al. (2011a). Briefly, the data reduction steps included: bias subtraction, flat-fielding, cosmic ray hit removal, building the wavelength solution using arc-line spectra, constructing the spectral line spread function (LSF) variation model using the twilight spectrum and night sky spectrum subtraction taking into account the LSF variation along and across the wavelength direction (Katkov & Chilingarian 2010), and adaptive binning along the slit in order to achieve the minimal value of the signal-to-noise ratio $S/N = 20$ per spatial bin.

We also used the data obtained with the integral-field spectrograph SAURON (Bacon et al. 2001) on the 4.2 m William Herschel Telescope. NGC 524 was observed in three positions of the SAURON lenslet array with $0.94''$ sampling (see Figure 1, left). The covered spectral range was 480–540 nm with the spectral resolution 0.48 nm. For our analysis we used the science-ready data cube kindly provided by E. Emsellem that we binned adaptively using Voronoi tessellation (Cappellari & Copin 2003) to the minimal S/N ratio of 100 per bin.

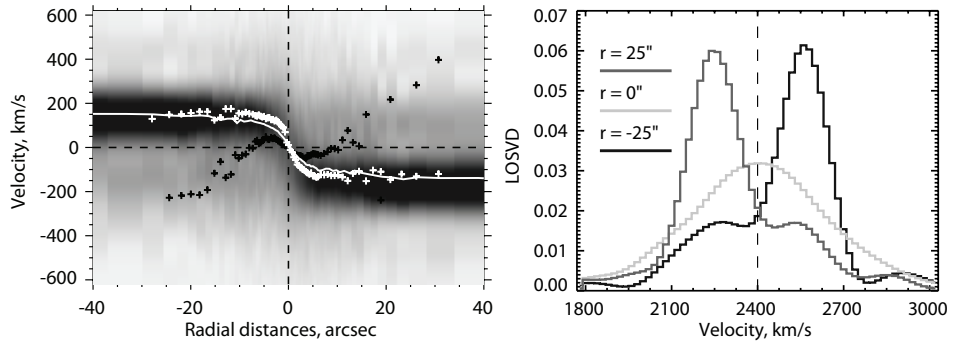

Fig. 2. Left panel. The position vs. velocity diagram. White line presents a radial velocity profile obtained using one-component model. Black and white crosses correspond to the 'bulge' and 'disk' components in the two-component model. Right panel. The LOSVD at the radii –25, 0 and 25 arcsec.

3. DATA ANALYSIS

3.1. SSP-equivalent parameters and emission-line kinematics

We derived the parameters of internal kinematics and stellar populations of NGC 524 by fitting high-resolution PEGASE.HR (Le Borgne et al. 2004) simple stellar population (SSP) models against our spectra using the NBURSTS full spectral fitting technique (Chilingarian et al. 2007a,b). We determined SSP-equivalent ages T and metallicities [Z/H] of the stellar population as well as the stellar kinematics using the Gauss-Hermite parametrization up to the 4th moment, i.e., v, σ, h_3 and h_4 (van der Marel & Franx 1993). The derived parametric LOSVD exhibits a strong asymmetry leading to the *non-physical* values of h_3 and $h4$ (see Figure 1, right) corresponding to significantly negative LOSVD "wings".

The emission-line spectrum at every spatial bin was obtained by the subtraction of the stellar contribution (i.e., the best-fitting model) from the observed spectrum. Then we fitted it with pure Gaussians convolved with the LSF in order to determine the kinematics of the ionized gas and emission-line ratios.

3.2. Non-parametric LOSVD

We propose a non-parametric recovery technique based on the full spectral fitting requiring no *a priory* LOSVD knowledge. The logarithmically rebinned model spectrum, $\mathcal{F}(\lambda)$ is the convolution of the assumed normalized LOSVD, $\mathcal{L}(v)$, with the rest-frame SSP model, $\mathcal{F}_r(w)$: $\mathcal{F}(w) = \int_{u_{\min}}^{u_{\max}} \mathcal{F}_r(w-u)\mathcal{L}(u)du$, where $w = \ln(\lambda)$, $u = \ln(1+v/c)$. We used the output SSP model of the NBURSTS fitting as a template spectrum $\mathcal{F}_r$. This equation can be considered as a linear inverse problem whose solution is very sensitive to the noise in the data. Hence, we chose to regularize the problem by requiring the LOSVD to be smooth. In order to do so, we use the cubic penalization $\mathcal{P}(\mathcal{L}) = \mathcal{L}^T \cdot \mathcal{D}^T \cdot \mathcal{D} \cdot \mathcal{L}$, where $\mathcal{D}$ is the third-order difference operator. The function to be minimized is given by $\chi^2 + \lambda\mathcal{P}(\mathcal{L})$. For discussion on the choice of λ see Press et al. (2007).

Using this technique, we confirmed a strong asymmetry of the NGC 524 LOSVD. Figure 2 displays the result of the LOSVD recovery for the long-slit data along the kinematical major axis as a position-velocity diagram (left panel). The LOSVD profiles at radii -25, 0 and 25 arcsec are shown to the right.

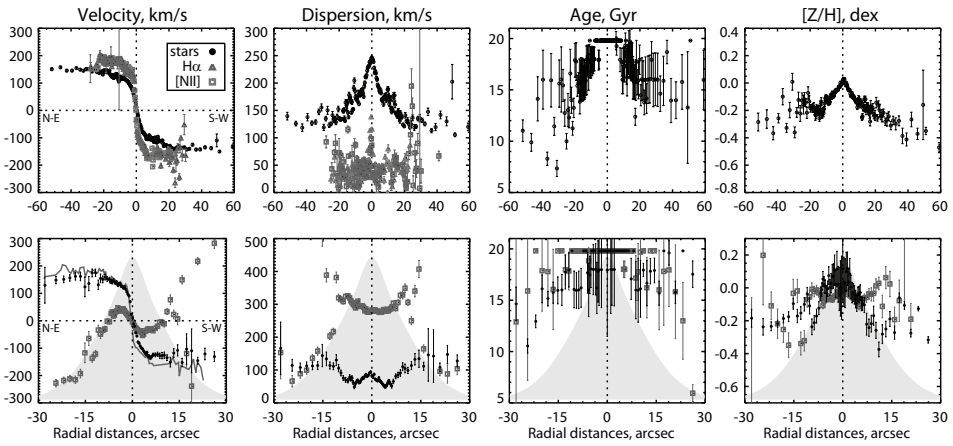

Fig. 3. SCORPIO long-slit spectroscopic data. Upper row: single component spectral fitting ($S/N = 20$) in the 'green' spectral domain. Lower row: two-component spectral fitting ($S/N = 40$). Black points and grey squares correspond to the 'disk' and 'bulge' components, respectively, the grey line shows the $H\alpha$ kinematics and the light grey shaded region presents a relative bulge contribution.

3.3. Two-component parametric LOSVD recovery

Another approach we use is a full spectral fitting using a two-component model where different stellar population components have two different pure Gaussian LOSVDs. An optimal template is represented by a linear combination of two SSPs characterized by their ages and metallicities, each of them convolved with its own Gaussian LOSVD.

We fit the data for NGC 524 using two SSPs. Our parametric fitting procedure may be used to determine relative contributions of SSP components, but here we fix them to the bulge plus the inner disk (1st SSP) and the outer disk (2nd SSP) components of the total light profile decomposition derived by Sil'chenko (2009).

4. RESULTS AND DISCUSSION

4.1. Kinematics

At all radii the LOSVD of NGC 524 clearly demonstrates the presence of at least two components clearly visible in Figs. 2–3 confirmed independently by the non-parametric and parametric LOSVD reconstruction on SAURON and SCORPIO datasets. The inner region of the galaxy, which corresponds to a small exponential pseudobulge identified by Sil'chenko (2009), is very hot in a dynamical sense with the velocity dispersion exceeding 300 $\mathrm{km\,s^{-1}}$.

This component disappears at about $R \approx 20''$, where we see a sharp drop in the velocity dispersion and radial velocities increasing outwards, suggesting the counter-rotation with respect to the main disk (see the bottom panels of Fig. 3). At the radii $R > 20''$, the LOSVD recovered non-parametrically also becomes strongly bi-modal with the secondary component clearly visible in Fig. 1.

4.2. Stellar populations and emission-line ratios

Radial variations of the stellar population parameters derived from the SSP

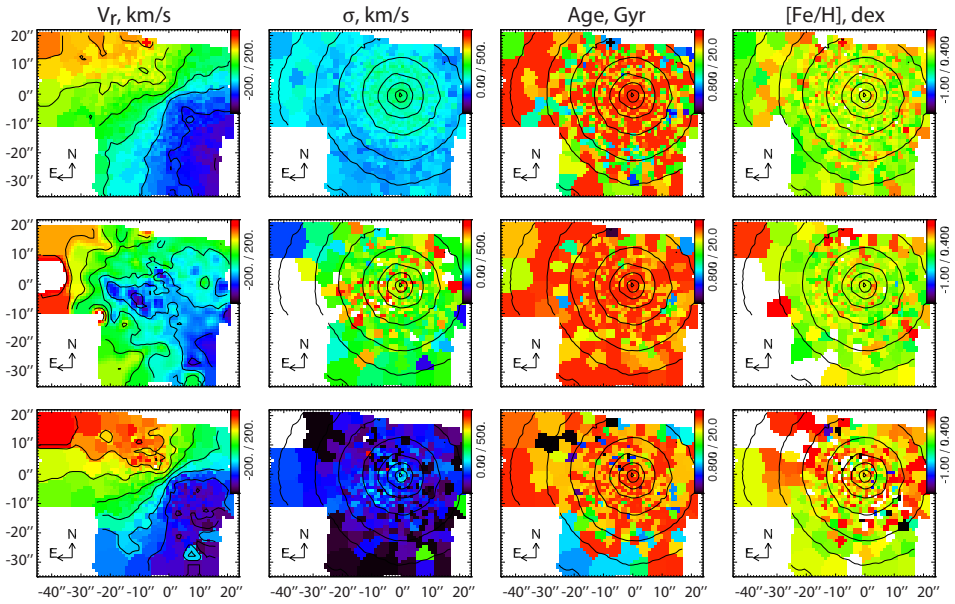

Fig. 4. SAURON integral-field spectroscopic data. From left to right: velocity, velocity dispersion, SSP-equvalent ages and metallicities. First row correspond to one-component fitting spectra. Second and third rows present the 'bulge' and 'disk' parameter maps for two-component spectra decomposition.

fitting of the long-slit data are shown in Figure 3 (right-top). The mean stellar age is very old ($T \gtrsim 15$ Gyr) being at the limit of the SSP model grid in the central 20″. The metallicity in the center is close to the solar value decreasing down to [Z/H] ≈ –0.4 dex in the outer disk. The spectrum fitting results using a two-component model are presented in Figure 3 (right-bottom). The 'bulge' (grey squares) and the 'disk' (black points) components do not have significant differences of the age radial profile being both very old with the 'bulge' reaching the limiting age in the models. The 'disk' metallicity decreases from [Z/H] ≈ 0.1 dex in the center to –0.2 dex at large radii. Our analysis of the virtually noiseless ($S/N > 100$) SAURON dataset (see Figure 4, right columns) agree with the long-slit data. The mean stellar parameters of the 'bulge' component are $T > 15$ Gyr and [Z/H] ≈ –0.1 dex, while for the 'disk' component they are $T \approx 14$ Gyr and [Z/H] ≈ 0.1 dex.

The analysis of emission-line ratios using the classical diagnostics [O III]/Hβ vs. [N II]/Hα (Baldwin et al. 1981) rules out the ongoing star formation in the disk of NGC 524 leaving the space for the shockwave excitation or the nuclear activity. However, the latter mechanism cannot explain the large spatial extent of the emission-line region.

4.3. Discussion

A very good agreement between the dynamically cold 'disk' component of the stellar LOSVD and the ionized gas kinematics suggest that the gas is rotating in the plane of the main stellar disk. A small discrepancy of the rotation (20 km s^{-1})

can be explained by the asymmetric drift and well corresponds to the observed stellar velocity dispersion of the disk component of ~ 100 km s^{-1}. Old stellar population and the emission-line diagnostics rule out both recent and ongoing star formation in the gaseous disk. The second kinematical component (Figure 3) probably corresponds to two different structures at different radii. The dynamically hot inner part without much rotation is a manifestation of the compact central pseudo-bulge, while at $R > 20''$ we see the presence of a counter-rotating disk component that is supported by the drops in the velocity dispersion (300 to < 100 km s^{-1}) and metallicity (0.0 to -0.3 dex) profiles.

The origin of NGC 524 has to be investigated in detail using state-of-art numerical simulations. Right now we can speculate about its evolution based on the observational results we have. NGC 524 might have originated from the face-on collision of two initially counter-rotating co-planar giant disk galaxies. The metallicity difference between the two components suggests the merger mass ratio of about 1:4. The gas in the main stellar disk of NGC 524 might have survived from the original galaxy or collected later from mergers with low-mass satellites. However, its surface density is still below the threshold and therefore it prevents the start of star formation.

ACKNOWLEDGMENTS. We thank the LOC for financial support and efficient organization of the conference. We are also grateful to Dr. Eric Emsellem, who provided the reduced SAURON data cube for NGC 524. This work was supported by the Russian Foundation for Basic Research (project No. 09-02-00870).

REFERENCES

Afanasiev V. L., Moiseev A. V. 2005, Astronomy Letters, 31, 193
Bacon R., Copin Y., Monnet G. et al. 2001, MNRAS, 326, 23
Baldwin J. A., Phillips M. M., Terlevich R. 1981, PASP, 93, 5
Cappellari M., Copin Y. 2003, MNRAS, 342, 345
Chilingarian I. V., Prugniel P., Sil'chenko O. K., Afanasiev V. L. 2007a, MNRAS, 376, 1033
Chilingarian I. V., Prugniel P., Sil'chenko O. K., Koleva M. 2007b, in *Stellar Populations as Building Blocks of Galaxies*, (IAU Symp. 241), eds. A. Vazdekis & R. F. Peletier, p. 175, arXiv:0709.3047
Emsellem E., Cappellari M., Peletier R. F. et al. 2004, MNRAS 352, 721
Garcia A. M. 1993, A&AS, 100, 47
Katkov I. Yu., Moiseev A. V., Sil'chenko O. K. 2011, accepted by ApJ = arXiv:1106.5323
Katkov I. Yu., Chilingarian I. V. 2011, in *Astronomical Data Analysis Software and Systems*, ASP Conf. Ser., eds. I. N. Evans et al., 442, p. 143 = arXiv:1012.4125
Le Borgne D., Rocca-Volmerange B., Prugniel P. et al. 2004, A&A, 425, 881
Macchetto F., Pastoriza M., Caon N. et al. 1996, A&AS, 120, 463
van der Marel R. P., Franx M. 1993, ApJ, 407, 525
Magrelli G., Bettoni D., Galletta G. 1992, MNRAS, 256, 500
Mulchaey J., Davis D., Mushotzky R., Burstein D. 2003, ApJS, 145, 39
Press W. H., Teukolsky S. A., Vetterling W. T., Plannery B. P. 2007, *Numerical Recipes: the Art of Scientific Computing*, 3rd ed., Cambridge Univ. Press
Sil'chenko O. K. 2000, AJ, 120, 741
Sil'chenko O. K. 2009, in *The Galaxy Disk in Cosmological Context* (IAU Symp. 254), eds. J. Andersen et al., p. 173
Simien F., Prugniel P. 2000, A&AS, 145, 263